Polymer-Based Devices for Optical Communications

Myung-Hyun Lee, Jung Jin Ju, Suntak Park, Jung Yun Do, and Seung Koo Park

Polymers are emerging as new alternative materials for optical communication devices. We developed two types of polymer-based devices for optical communications. One type is for ultra high-speed signal processing that uses nonlinear optical (NLO) polymers in such devices as electro-optic (EO) Mach-Zëhnder (MZ) modulators and EO 2×2 switches. The other is for WDM optical communications that use low-loss optical polymers in such devices as 1×2, 2×2, 4-arrayed 2×2 digital optical switches (DOSs) and 16×16 arrayed waveguide grating (AWG) routers. For these devices, we synthesized a polyetherimide-disperse red 1 (PEI-DR1) side chain NLO polymer and a low-loss optical polymer known as fluorinated polyaryleneethers (FPAE). This paper presents the details of our development of these polymeric photonic devices considering all aspects from materials to packaging.

Manuscript received Dec. 13, 2001; revised Mar. 16, 2002.

Myung-Hyun Lee (phone: +82 42 860 5243, e-mail: mhl@etri.re.kr), Jung Jin Ju (e-mail: jjju@etri.re.kr), Suntak Park (e-mail: spark@etri.re.kr), Jung Yun Do (e-mail: jydo@etri.re.kr), and Seung Koo Park (e-mail: skpark@etri.re.kr) are with Wideband Photonics Device Team, ETRI, Daejeon, Korea.

I. INTRODUCTION

There are three approaches to high capacity optical transmission systems. The first is to decrease the channel spacing for wavelength division multiplexing (WDM) systems, the second is to increase the channel bit rate for time division multiplexing (TDM) systems, and the third is to extend the transparent spectral range in optical fiber. For WDM and TDM systems, a variety of optical devices are indispensable. Nowadays, the materials used are mostly inorganic, for example, InP, $LiNbO_3$, and silica.

Polymers are emerging as materials for optical devices because of their promising potential. Polymers for optical devices can be divided into two categories: one is for high speed signal processing in TDM systems and the other is for WDM optical communications. In the past decade, many researchers have studied the Mach-Zëhnder (MZ) modulator [1]-[14] and the 2×2 electro-optic (EO) switch [15]-[18] which use nonlinear optical (NLO) polymers for high speed and wide-band signal processing. In addition, a variety of devices, such as polarization controllers [19], second-harmonic generators [20], optical frequency converters [21], and photonic sensors [22] have also been investigated. In the areas of high speed and broad bandwidth, such devices have significant advantages over inorganic devices, such as $LiNbO_3$, or compound semiconductor devices. Such advantages are due mainly to the polymer's low dielectric constant, low optical dispersion, and fast electronic response in the range from low frequency to optical frequency. Other investigations have used low-loss optical polymers [23] for WDM systems, such as digital optical switches (DOSs) [24]-[28], tunable Bragg wavelength filters [29], variable optical attenuators (VOA) [30], and arrayed waveguide grating (AWG) multiplexer/

demultiplexers [31]-[33]. These devices have significant advantages over inorganic devices, such as silica devices, in the areas of planar lightwave circuits (PLC). Such advantages are due mainly to the ease of device fabrication and the great flexibility of the device structure. In addition, a low-loss polymer has a larger thermo-optic (TO) coefficient than silica.

We used NLO polymers and low-loss optical polymers to develop two types of polymer-based devices for optical communications. We report in detail our development of these polymeric photonic devices considering every aspect from materials to packaging.

II. MATERIALS

We synthesized a polyetherimide-disperse red1 (PEI-DR1) side-chain EO polymer to use as an NLO material (Fig. 1). The number-average molecular weight (M_n) was about 10,500 g/mol, and the M_w/M_n was 1.6, where M_w is the weight-average molecular weight. The glass transition temperature (T_g) was about 173 °C. For our NLO devices, we used UFC150 from Uray Co. for the lower cladding material and Resole HM2 from Koron Co. for the upper cladding material. We measured the EO coefficients using a simple reflection technique [34] at optical communication wavelengths, 0.83 μm, 1.3 μm, and 1.55 μm. Figure 2 gives the measured EO coefficients (r_{33}) of the poled sample with different poling fields. For the poling, the sample was heated to 173 °C, and DC voltage was applied. Unexpectedly, the value of r_{33} at 1.55 μm was bigger than the values at 0.83 μm and 1.3 μm. The refractive indices were measured using a prism coupler for transverse electric (TE) and transverse magnetic (TM) polarized light. Table 1 lists the measured refractive indices of PEI-DR1 (Core), UFC150 (lower clad), and Resole HM2 (upper clad) at 0.83 μm, 1.3 μm, and 1.55 μm wavelengths. The propagation losses of the PEI-DR1 slab waveguide were measured at 0.83 μm, 1.3 μm, and 1.55 μm with the TE- and TM-polarized light using the immersion technique [35]. For the measurement of the propagation losses, we prepared the sample with a slab waveguide on a substrate. The PEI-DR1 layer, with a thickness of 3.2 μm, was spin-coated on the UFC150 layer, which was 2 μm thick, for the lower cladding layer. The substrate for the slab waveguide had a thin Au electrode layer on a Si wafer. The results are tabulated in Table 2. The effects of the metallic loss caused by the gold electrode increased with a lengthening

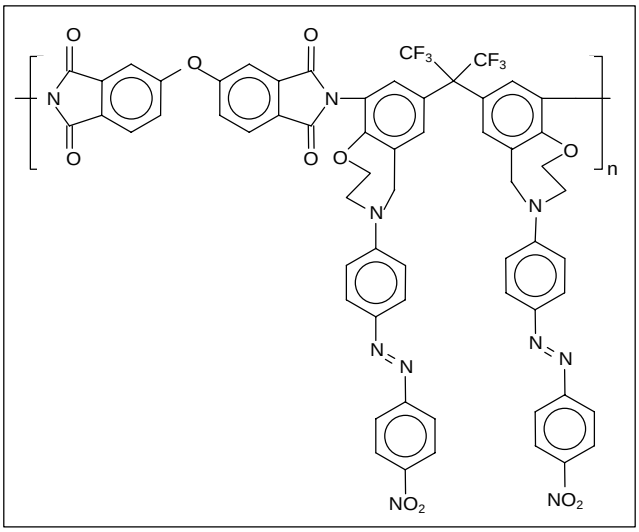

Fig. 1. Chemical structure of PEI-DR1.

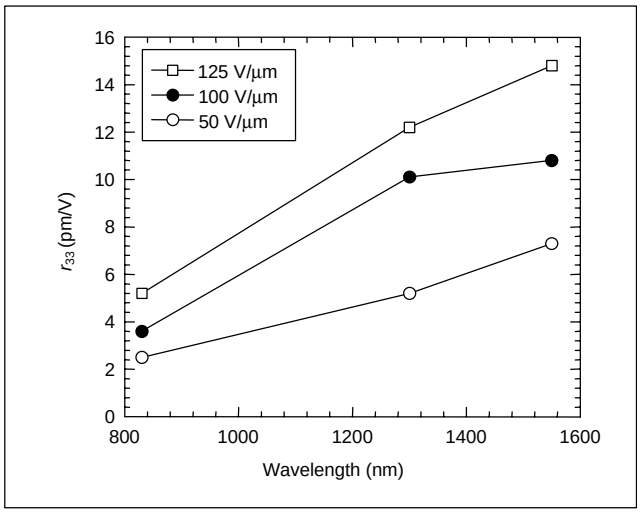

Fig. 2. r_{33} as functions of wavelength and poling field.

Table 1. Refractive indices.

	UFC150		PEI-DR1		R-HM2	
λ (μm)	n_{TE}	n_{TM}	n_{TE}	n_{TM}	n_{TE}	n_{TM}
0.83	1.5074	1.5088	1.6946	1.6874	1.6355	1.6337
1.3	1.5048	1.5069	1.6664	1.6607	1.6344	1.6333
1.55	1.5035	1.5055	1.6564	1.6499	1.6313	1.6309

Table 2. Propagation losses of slab waveguides.

Wavelength (μm)	TE0 (dB/cm)	TM0 (dB/cm)
0.83	0.91	0.94
1.3	1.70	1.77
1.55	2.2	3.0

wavelength. At 1.55 μm, the propagation loss was mostly caused not only by the gold electrode but also by the content of the C-H bond in the PEI-DR1. The other characteristics of our NLO materials are explained in [18].

For a low loss polymer, we synthesized fluorinated polyaryleneethers (FPAE) with thermally crosslinkable ethynyl phenol (EP) groups (FPAE-EP) at the end of the chain (Fig. 3(a)). The M_n of the FPAE-EP was about 8,940 g/mol, and the M_w/M_n was 1.56. We also synthesized FPAE-EP with resorcinol in the backbone (FPAE-RC-EP) (Fig. 3(b)). The M_n of the FPAE-RC-EP was 8,680 g/mol, and the M_w/M_n was 1.61. In designing and fabricating single-mode waveguide devices, it is important to control the refractive indices of the core and cladding materials. Figure 4 shows the dependence of the refractive indices for TE and TM mode polarization with the relative FPAE-RC-EP content in the copolymers at a 1.55 μm wavelength. The refractive index of the blended polymer increased as the FPAE-RC-EP content increased. Figure 4 reveals that the refractive index of polymers can be controlled by blending the ratio between the two polymers. The birefringence, which is the difference between n_{TE} and n_{TM}, was almost constant at low values of 0.003-0.004. To measure the optical propagation loss of the core polymer, we prepared a planar waveguide structure by coating the core and the cladding materials on a 2 μm-thick oxide layer on a Si substrate (Fig. 5(b)). We again measured the optical propagation loss using the high-index liquid immersion technique [35]. With the output power variation depending on the immersion distance as shown in Fig. 5(a), the losses were 0.28 dB/cm and 0.26 dB/cm for the TE and TM modes at a wavelength of 1.55 μm. The other characteristics of polymeric low-loss materials are explained in [36].

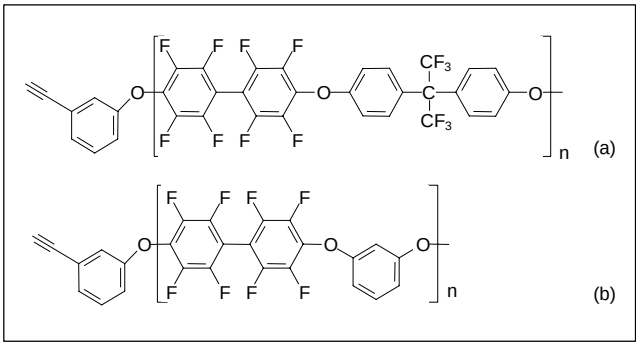

Fig. 3. Chemical structures of (a) FPAE-EP and (b) FPAE-RC-EP.

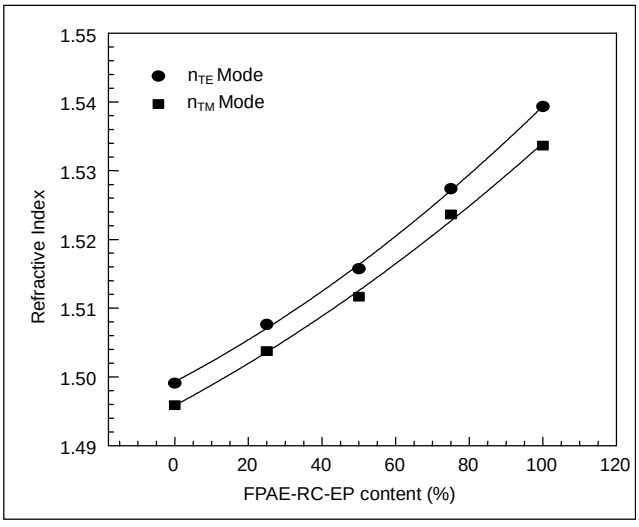

Fig. 4. Dependence of refractive index on FPAE-RC-EP content of blended polymers for TE and TM polarizations at a wavelength of 1.55 μm.

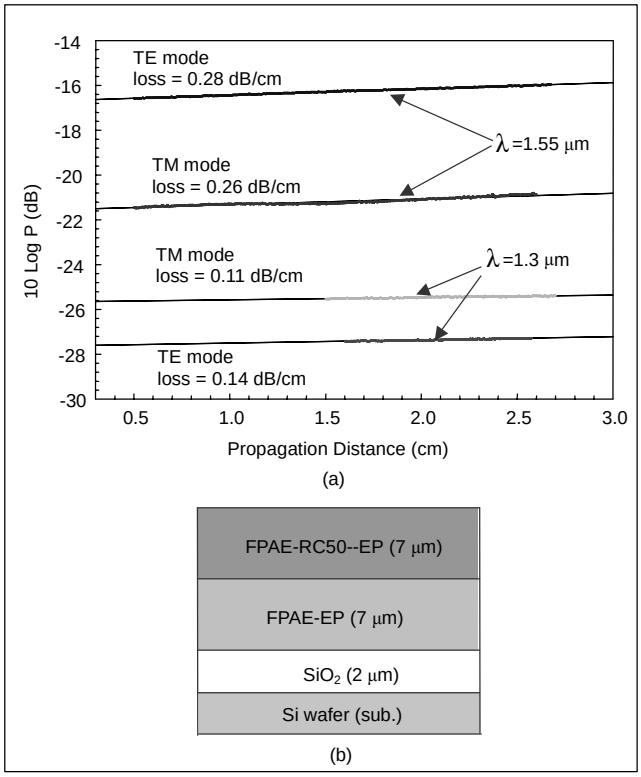

Fig. 5. (a) Optical attenuation profile in a slab waveguide and (b) cross-section view of the measured specimen.

III. FABRICATION

1. EO Devices

Our devices conventionally have a three-layer stack structure with a rib optical waveguide. The Cr/Au metallic layers were thermally evaporated and patterned as a bottom electrode on a 2 μm silica-coated Si wafer. The UFC 150 solution was spin-coated and UV-cured for the lower cladding layer with a thickness of 2 μm. Onto that, the PEI-DR1 solution was spin-coated and thermally-cured as the core layer with a thickness of

3.2 μm, and then the core layer was ion-etched with an etching depth of 0.5 μm for laterally confining the guided light. The Resole HM2 solution was also spin-coated and thermally-cured for the upper cladding layer with a thickness of 2 μm, and then Cr/Au was thermally evaporated for the top and the poling electrode. The Cr thin metallic layer was used as an adhesive. Electrode contacting poling was performed at 173 °C on a hot plate with a DC voltage of 1100 V (the poling field about 150 V/μm). The electrode was then patterned and electroplated. The thickness of the electroplated gold was properly controlled in the range of 3-6 μm by adjusting the electroplating time and current density. Finally, the opto-chip end faces were prepared by cleaving and polishing and then pig-tailed with V-groove arrayed optical fibers using an epoxy welding technique. K-connectors were connected for high frequency performance.

2. Low-Loss Devices

The low-loss device was fabricated on a 3-inch Si wafer. The cladding FPAE-EP polymer was spin-coated and cured at 250 °C for the lower cladding layer with a thickness of 11 μm. The core FPAE-RC(50)-EP polymer, for which the blending ratio of FPAE-EP and FPAE-RC-EP was 50:50, was spin-coated and cured at 250 °C for the core layer with a thickness of 6 μm. An O_2 reactive ion etching (RIE) process was used to form the proposed waveguide structure by standard photolithography. The cladding FPAE-EP polymer was spin-coated and cured at 250 °C for the upper cladding layer with a thickness of 11 μm. Finally, the thermal control electrode was evaporated and partially electroplated. The opto-chip was prepared by dicing, and the opto-chip end faces were polished and then pig-tailed with V-groove arrayed optical fibers using an epoxy welding technique. Gold-wire bonding was used for the thermal control electrodes.

IV. RESULTS OF NLO DEVICES

1. EO Modulator

Designing a polymeric MZ waveguide EO modulator for photonic applications requires a single mode operation. This can be achieved by controlling the width and thickness of the guiding layer and the etching depth in the rib waveguide structure. For single mode operation, the rib waveguide dimensions, *W, T, H*, as defined in Fig. 6, have to fulfill the following two equations [37],

$$\frac{T}{H} \geq 0.5 \qquad (1)$$

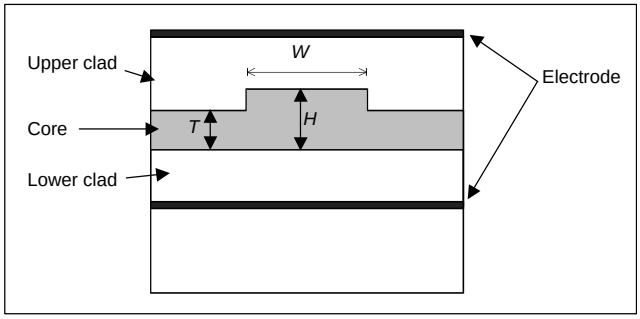

Fig. 6. Cross-section of rib waveguide.

$$\frac{W}{H} \leq 0.3 + \frac{T/H}{\sqrt{1-(T/H)^2}}. \qquad (2)$$

Considering these factors, we designed the waveguide for single mode operation with dimensions of W = 4 μm, T = 2.7μm, and H = 3.2 μm. The total waveguide length of the MZ modulator from the input to the output was 22 mm, the waveguide length of the interferometer arm was 15 mm, the branching angle in the Y-branch was 1 degree, and the distance between the two arms was 25 μm. The electrode consisted of a microstrip line and tapered coplanar pads (Fig. 7(a)). The performance of our optically and electrically packaged device as shown in Fig. 8(a) was as follows: the half wave voltage was 11 $V_{p\text{-}p}$, the extinction ratio was 23 dB (Fig. 9(a)), and

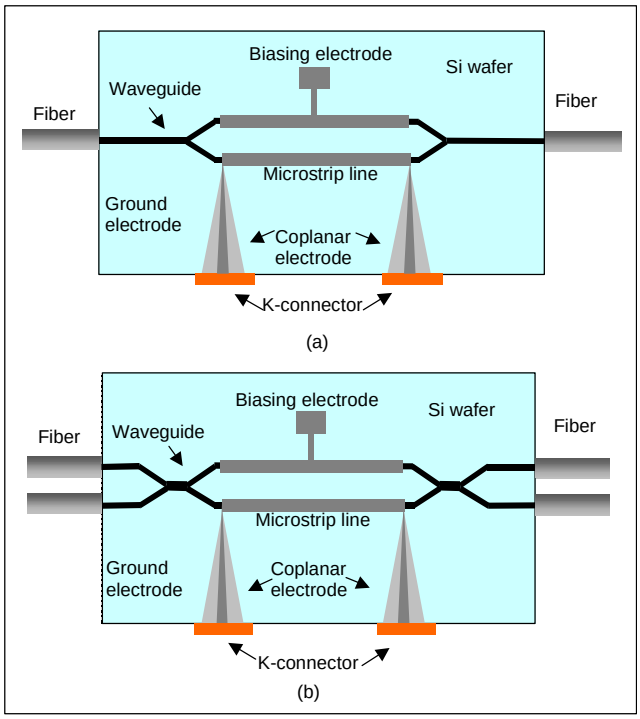

Fig. 7. Schematic views of (a) the Mach-Zëhnder Modulator and (b) the EO 2×2 switch.

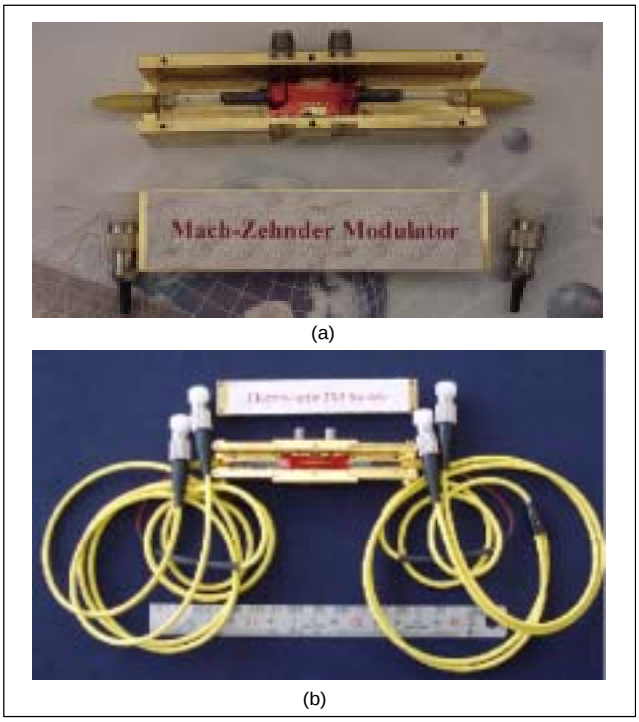

Fig. 8. Photographs of the packaged (a) Mach-Zëhnder Modulator and (b) 2×2 switch.

the fiber to fiber optical loss was 15 dB at λ = 1.3 μm. The bandwidth was tested up to 2.5 GHz.

2. EO 2×2 Switch

We fabricated the electrically and optically packaged polymeric EO 2×2 switch for high-speed optical communications [18]. The switch consisted of a MZ interferometer and modified bifurcation optically active (MBOA) waveguides [17] (Fig. 7(b)). The design of our switch fundamentally used a single mode operation. However, the two lowest order modes are required in the straight channel regions of an MBOA waveguide structure switch. This can be achieved by controlling the width and thickness of the guiding layer and the etching depth in the rib waveguide structure. For the single mode operation, the rib waveguide dimensions, *W, T, H*, as defined in Fig. 6, have to fulfill (1) and (2). For the two mode operation, they do not have to fulfill the two equations. Considering these factors, we designed the waveguide for a single-mode operation with dimensions of $W = 4$ μm, $T = 2.7$ μm, and $H = 3.2$ μm and the waveguide for a two-mode operation with dimensions of $W = 8$ μm, $T = 2.7$ μm, and $H = 3.2$ μm. In the MZ interferometer region of the MBOA structure, a single microstrip line with a length of 15 mm was fabricated onto one arm of the MZ interferometer. We used a tapered quasi coplanar waveguide and a K-connector to couple

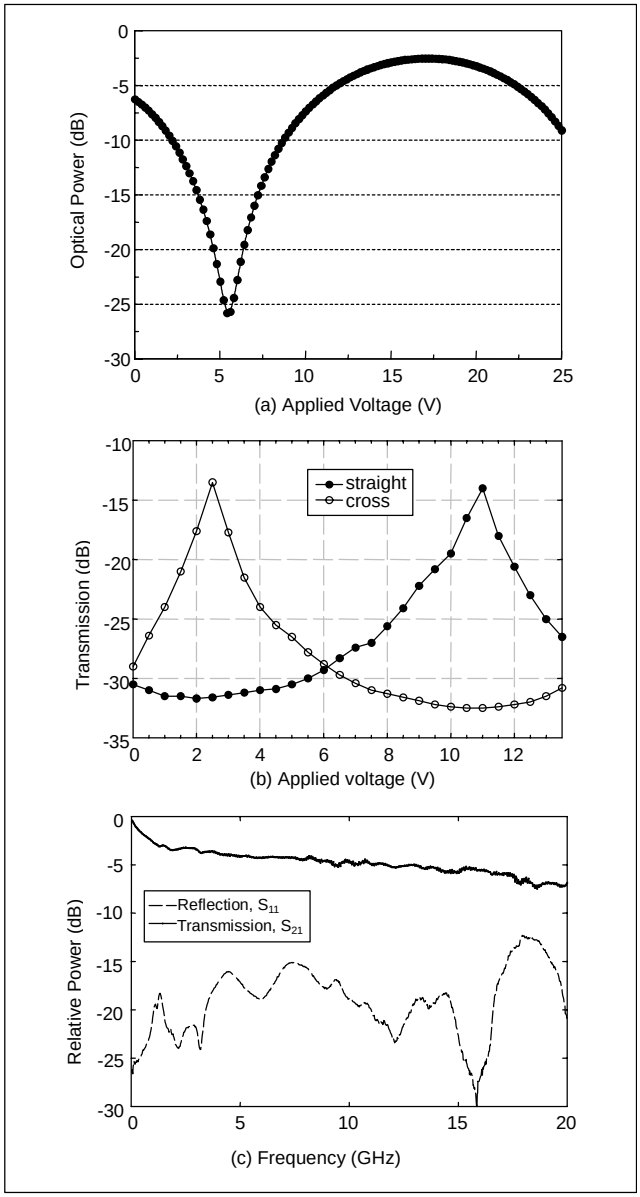

Fig. 9. Measured optical transmittances of (a) Mach-Zëhnder Modulator, (b) 2×2 switch at 1.3 μm, and (c) RF power losses versus frequency.

the radio frequency (RF) input power (Fig. 7(b)). The performance of the optically and electrically packaged device (Fig. 8(b)) was as follows: the crosstalk of the cross arm was –18.1 dB and that of the straight arm was –18.5 dB with an operating voltage of 8.5 V (Fig. 9(b)). The measured optical loss was 14 dB at λ = 1.3 μm. The 6-dB attenuation in RF transmission corresponded to about 17 GHz (Fig. 9(c)).

V. RESULTS OF LOW-LOSS DEVICES

1. 1×2, 2×2, 4-Arrayed 2×2 Digital Optical Switches (DOSs)

We designed and fabricated 1×2, 2×2, 4-Arrayed 2×2

DOSs using fluorinated polymers. Figure 10(a) shows a schematic view of a 2×2 DOS consisting of four 1×2 DOS elements. This waveguide structure is the same as that in [28]. The branching angle (α) of the 1×2 DOS was about 0.13° at the Y-branch regions and the cross angle (β) between the two waveguides was 27 degrees at the center point. However, the outside four electrodes at the 2×2 DOS element were connected and the inside four electrodes were also connected (Fig. 10(a)). The connected regions at the electrodes were electroplated so that they would not become a heating element. If voltage is applied to the inside electrode, the temperature in the inside of the connected Y-branches will increase to lower the refractive indices but the refractive indices in the outside of the connected Y-branches will increase correspondingly. Therefore, the lights input to the light input portions in1 and in2 go out to the light output portions out1 and out2, respectively. If voltage is applied to the outside electrode, the temperature in the outside of the connected Y-branches will increase to lower the refractive indices but the refractive indices in the inside of the connected Y-branches will increase correspondingly. Therefore, as the lights input to the light input portions in1 and in2 cross, they go out to the light output portions out2 and out1, respectively. Figures 11(a) and (b) show photographs of the optically and electrically packaged 1×2 and 2×2 DOSs, respectively. Figures 12(a) and (b) show the transmission characteristics of the 1×2 and 2×2 DOSs. The performance of the 1×2 DOS (Fig. 11(a)) was as follows: the operating wavelength range was 1520-1560 nm, the total insertion loss was less than 2.5 dB, the crosstalk less than 25 dB, the

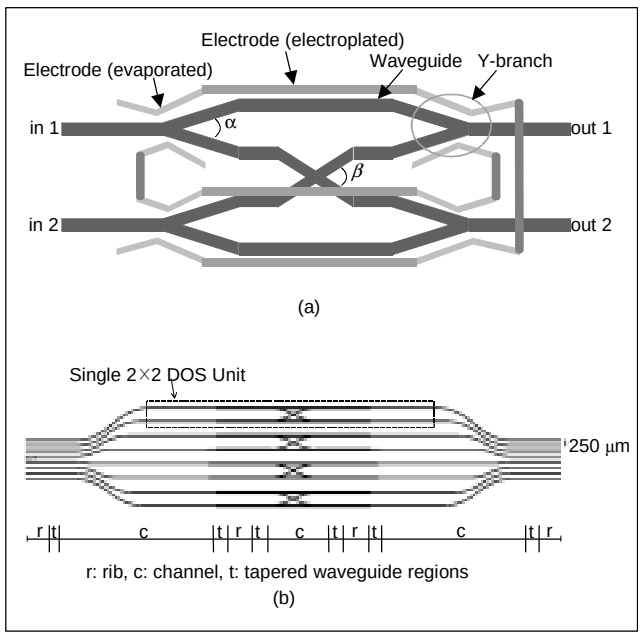

Fig. 10. Schematic views of (a) a single 2×2 DOS and (b) 4-arrayed 2×2 DOS waveguides.

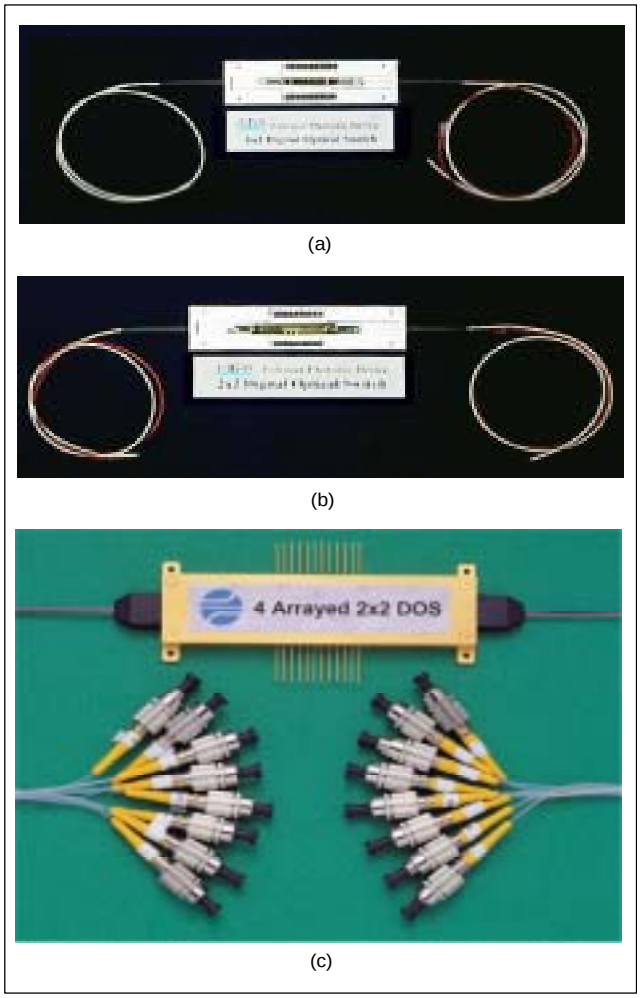

Fig. 11. Photographs of the packaged (a) 1×2 DOS, (b) 2×2 DOS, and (c) 4-arrayed 2×2 DOS.

polarization dependent loss (PDL) less than 0.2 dB, the switching time less than 3 ms, the operation electrical power less than 100 mW, and the operation voltage was about 3-5 V. The performance of the 2×2 DOS (Fig. 11(b)) was as follows: the operating wavelength range was 1520-1560 nm, the total insertion loss was less than 3.5 dB, the crosstalk less than 30 dB, the PDL less than 0.3 dB, the switching time less than 3 ms, the operation electrical power less than 300 mW, and the operation voltage was about 6-10 V. Figure10(b) shows a schematic view of the 4-arrayed 2×2 DOS. The separation width at 8 input/output waveguides was 250 μm for pig-tailing once, and the bending radius (R) at the outside 2×2 DOS elements was 10 mm. The chip size of the 4-arrayed 2×2 DOS was 45×12 mm^2.

The rib waveguides at the Y-branch regions were designed to increase coupling efficiency, that is to say, to increase the interaction of the separated modes laterally. Also, the rib waveguides at the input/output ports were designed to decrease coupling loss with optical fibers to create a large mode size.

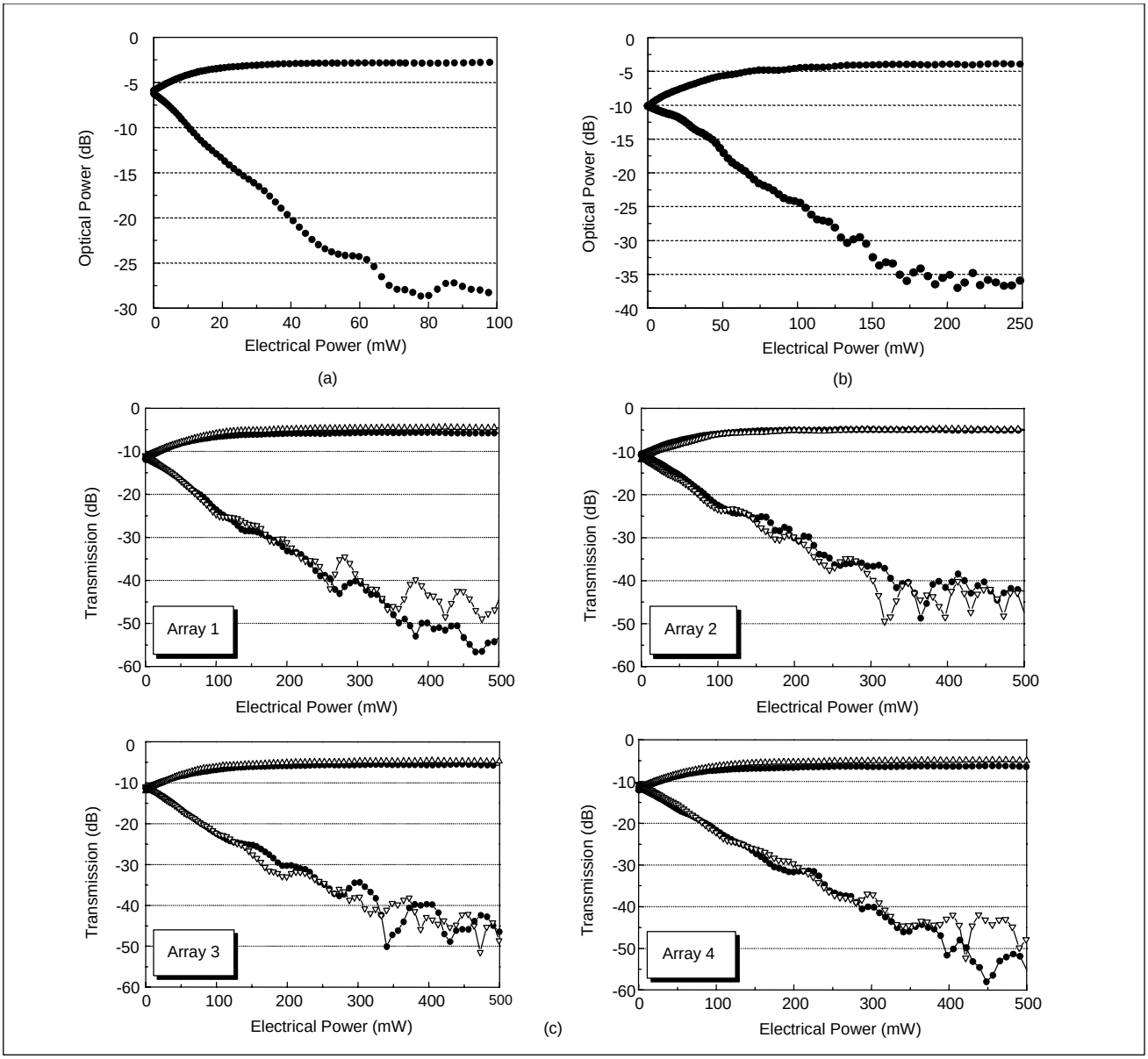

Fig. 12. Transmission characteristics of (a) 1×2 DOS, (b) 2×2 DOS, and (c) 4-arrayed 2×2 DOS.

The channel waveguides at the bending regions were designed to decrease the total thickness for lowering the electrical power. We could also reduce the total length by using the high index difference channel waveguides with large bending radius. The rib waveguide and the channel waveguide were connected by a vertically tapered waveguide (Fig. 13). Figure 11(c) shows photographs of the optically and electrically packaged 4-arrayed 2×2 DOS. Figure 12(c) shows the transmission characteristics of the 4-arrayed 2×2 DOS elements. The performance of the 4-arrayed 2×2 DOS (Fig. 12(c)) was as follows: the crosstalk was less than – 30 dB for all the 4-arrayed 2×2 DOS elements when a total electrical power of 250 mW was applied to the thin metal heaters. The deviation of the crosstalks was ± 2 dB at 250 mW. The PDL was 0.5 dB, 0.2 dB, 0.5 dB, and 0.7 dB for the first, second, third, and fourth 2×2 DOS elements, respectively. The falling and rising times were less than 5 msec. The total insertion losses ranged from 3.5 to 4.0 dB.

2. AWG Router

We designed a polymeric 16×16 AWG router with a 0.8 nm (100 GHz) channel spacing operating at 1550 nm. The AWG router is shown schematically in Fig. 14. It consisted of dispersive arrayed waveguides connected to 16 input waveguides and 16 output waveguides through two concave slab waveguides designed in a Rowland circle configuration. Input and output waveguides were fanned out to a pitch of 250

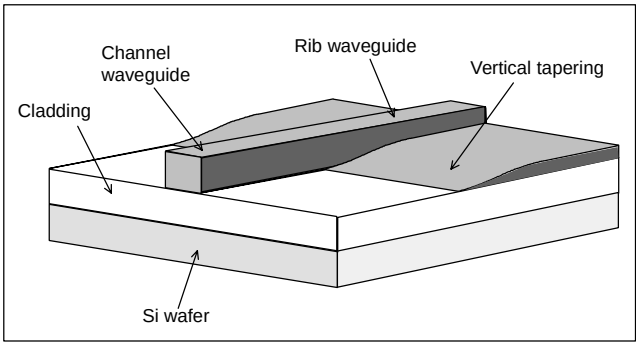

Fig. 13. Schematic view of a portion where the rib waveguide and the channel waveguide are connected by the vertically taped waveguide.

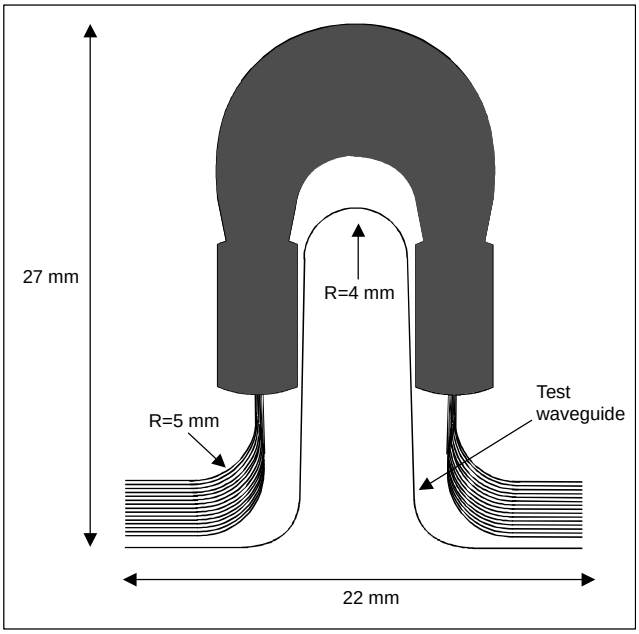

Fig. 14. Schematic view of 16×16 AWG router with 0.8 nm (100GHz) channel spacing.

μm for pig-tailing to a fiber ribbon. To minimize the coupling loss with optical fiber and to obtain a lateral single mode condition, we made the channel waveguide of the AWG router as a rib type at the input and output ports. The rib waveguide was connected to the buried type channel waveguide adiabatically by a vertical tapering (Fig. 13). The core size and refractive index difference of (Δ) the channel waveguide were 6×6 μm^2 and 1%, respectively. With this core size, the channel waveguide was weakly double mode guiding. We chose the large core size because the propagation loss due to the sidewall roughness of the waveguide increased as the refractive index difference became larger [38]. This might also possibly increase the phase error in the arrayed waveguides. The bending radius in the array varied from 4 to 7.5 mm and the minimum waveguide separation was 20 μm. We included the

Table 3. Design parameters of a 16×16 AWG router.

Parameter	Symbol	Value
Center wavelength	λ_c	1550 nm
Channel spacing	Δf_{ch}	0.8 nm (100 GHz)
Focal length of slab waveguide	R_a	6161 μm
Number of arrayed waveguides	N_a	131
Path difference of arrayed waveguides	ΔL	125 μm
Diffraction order	m	120
Free spectral range	Δf_{FSR}	1600 GHz
Group index	N_g	1.49709
Effective refractive index of channel	N_{eff} (channel)	1.48941
Effective refractive index of slab	N_{eff} (slab)	1.49221
Minimum curvature	R_{min}	4 mm

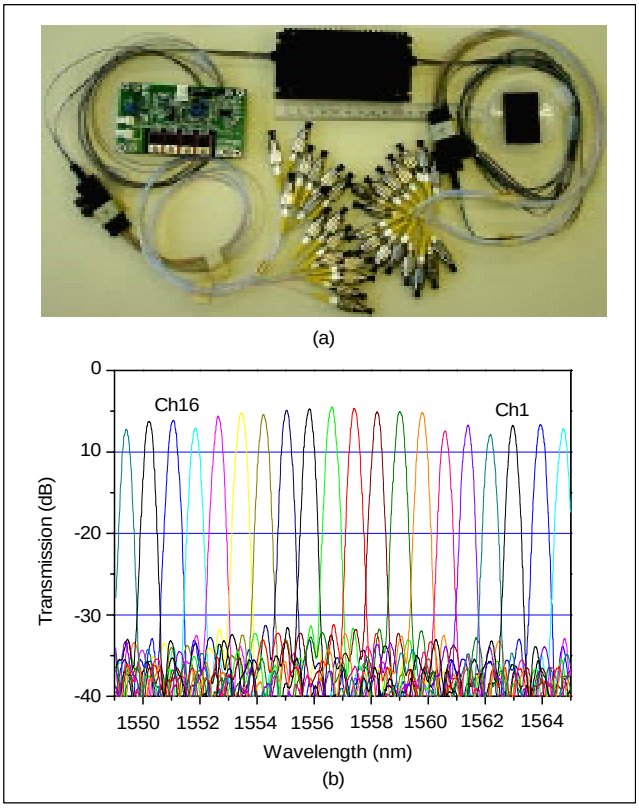

Fig. 15. (a) Photograph of the packaged 16×16 AWG router and (b) transmission spectra overlay of the AWG router.

curved test waveguides to evaluate the origins of the chip losses. The occupied area of the phase array was 15×11 mm^2 and the device size was 27×22 mm^2. Table 3 lists the detailed design parameters. Figure 15(a) shows a photograph of a fully packaged 16×16 AWG Router. Figure 15(b) shows the

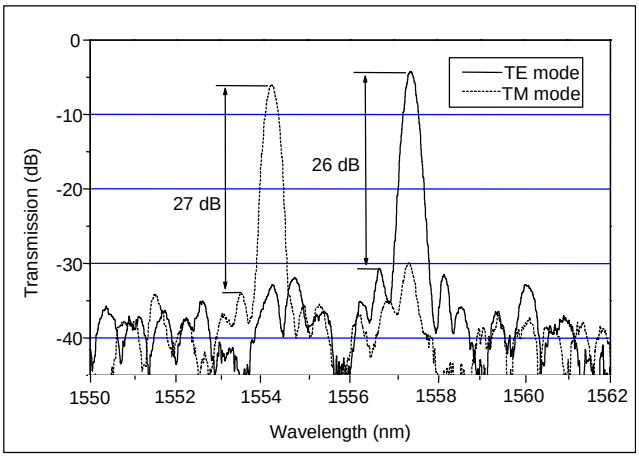

Fig. 16. The transmission spectra for the TE and TM modes measured with 8th input and 8th output ports.

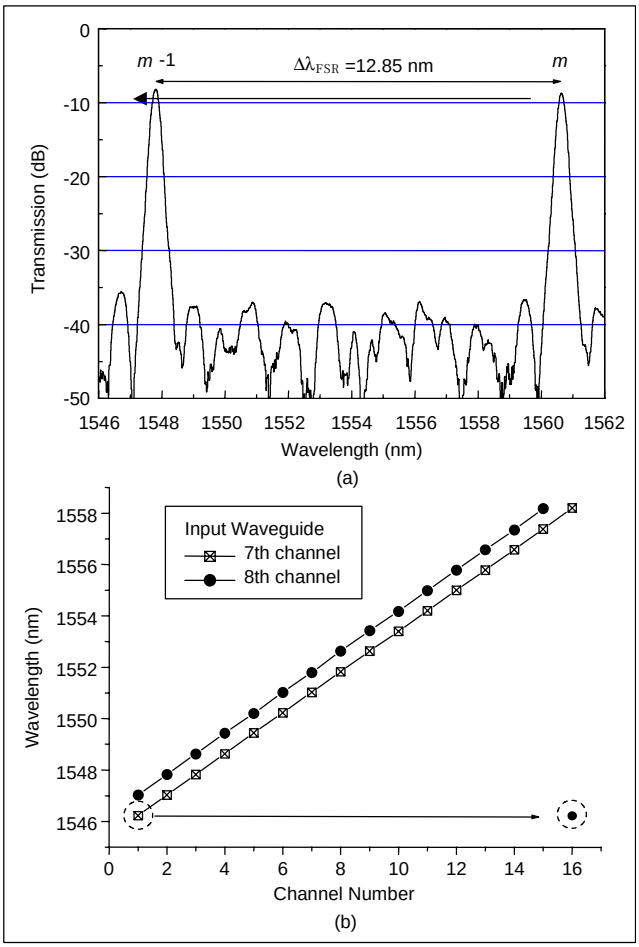

Fig. 17. (a) Free spectral range characteristics of AWG for light input to port 7 and measured at output port 16. (b) The measured pass wavelengths of the 16×16 AWG router output channels. The slopes are 0.796 nm/channel and 0.795 nm/channel for 7th and 8th input port, respectively.

measured transmission spectra of the 16 output channels around the 1550 nm wavelength, as measured with TE polarized light injected into the 8th input port. The output power uniformity over the 16 channels was about 3.2 dB. However, we could improve the power uniformity by controlling the polarization and temperature whenever we measured the device. The fiber to fiber insertion loss of the center channel was 4.8 dB. The 1 and 3 dB passband widths of the transmission spectrum were 0.13 and 0.22 nm, respectively. The channel crosstalks were less than –26 and –27 dB for TE mode and TM mode, respectively (Fig. 16). Figure 16 shows the transmission spectra for the TE and TM modes. The polarization dependent peak shift was 3.25 nm. The peak wavelength shift between the TE and TM modes was due to the material birefringence induced by the difference of the refractive index between the TE and TM modes. Figure 17(a) shows the free spectral range (FSR) of the AWG router. The wavelength difference from the transmission peak of order m-1 and that of order m was 12.85 nm, which is nearly 16 times the channel spacing, 0.8 nm. To test the cyclic rotation properties of the output channels, we measured the pass wavelengths when the light was launched into either channel 7 or 8 (Fig. 17(b)). The output wavelengths with the 7th input channel shifted nearly by 0.8 nm and appeared at the adjacent channels when the input channel changed to the 8th. The wavelength of the 1st channel with the 7th input waveguide showed at the 16th channel with the 8th input waveguide. During the channel shift, the error of the peak wavelength was smaller than 0.03 nm for all 16 channels. Figure 17(b) shows the slopes at 0.796 nm/channel and 0.795 nm/channel for the 7th and 8th input ports, respectively, which were almost the same as the designed spacing of 0.8 nm/channel.

VI. CONCLUSION

In this study, we synthesized PEI-DR1 side chain NLO polymers for ultra high-speed signal processors and FPAE low-loss optical polymers for WDM optical communications. We fabricated EO MZ modulators and EO 2×2 switches using PEI-DR1 polymers. With the developed the EO polymer, we produced the high speed and broad bandwidth devices easily and cost-effectively by using the polymer's unique properties of a low dielectric constant and low dielectric dispersion. We also fabricated 1×2, 2×2, 4-arrayed 2×2 DOSs, and 16×16 AWG routers using FPAE low-loss optical polymers. With the developed low-loss optical polymers, we produced the waveguide devices of high performance easily and cost-effectively by using the low-loss polymer's properties of good processibility, easy controllability of the refractive index, and the large TO coefficient.

REFERENCES

[1] D.G. Girton, S.L. Kwiatkowski, G.F. Lipscomb, and R.S. Lytel,

"20 GHz Electro-Optic Polymer Mach-Zëhnder Modulator," *Appl. Phys. Lett.*, vol. 58, no. 16, 1991, pp. 1730-1732.

[2] E. Van Tomme, P. Van Daele, R. Baets, G.R. Mohlmann, and M.B.J. Diemeer, "Guided Wave Modulators and Switches Fabricated in Electro-Optic Polymers," *J. Appl. Phys.*, vol. 69, no. 9, 1991, pp. 6273-6276.

[3] C.C. Teng, "Traveling-Wave Polymeric Optical Intensity Modulator with More Than 40 GHz of 3-dB Electrical Bandwidth," *Appl. Phys. Lett.*, vol. 60, no. 13, 1992, pp. 1538-1540.

[4] M. Hikita, Y. Shuto, M. Amano, R. Yoshimura, S. Tomaru, and H. Kozawaguchi, "Optically Intensity Modulation in a Vertically Stacked Coupler Incorporating Electro-Optic Polymer," *Appl. Phys. Lett.*, vol. 63, no. 9, 1993, pp. 1161-1163.

[5] M.H. Lee, H.J. Lee, S.G. Han, H.Y. Kim, K.H. Kim, Y.H. Won, and S.Y. Kang, "Fabrication and Characterization of an Electro-Optic Polymer Waveguide Modulator for Photonic Applications," *Thin Solid Films*, vol. 303, 1997, pp. 287-291.

[6] Y. Shi, W. Wang, J.H. Bechtel, A. Chen, S. Garner, S. Kalluri, W.H. Steier, D. Chen, H.R. Fetterman, L.R. Dalton, and L. Yu, "Fabrication and Characterization of High-Speed Polyurethane-Disperse Red 19 Integrated Electrooptic Modulators for Analog System Applications," *IEEE J. Selected Topics in Quantum Electron.*, vol. 2, no. 2, 1996, pp. 289-299.

[7] D. Chen, H.R. Fetterman, A. Chen, W.H. Steier, L.R. Dalton, W. Wang, and Y. Shi, "Demonstration of 110 GHz Electro-Optic Polymer modulators," *Appl. Phys. Lett.*, vol. 70, no. 25, 1997, pp. 3335-3337.

[8] W.H. Steier, A. Chen, S.S. Lee, S. Garner, H. Zhang, V. Chuyanov, L.R. Dalton, F. Wang, A.S. Ren, C. Zhang, G. Todorova, A. Harper, H.R. Fetterman, D. Chen, A. Udupa, D. Bhattacharya, and B. Tsap, "Polymer Electro-Optic Devices for Integrated Optics," *Chem. Phys.*, vol. 245, 1998, pp. 487-506.

[9] D. Chen, D. Bhattacharya, A. Udupa, H.R. Fetterman, A. Chen, S.S. Lee, J. Chen, W.H. Steier, and L.R. Dalton, "High-Frequency Polymer Modulators with Integrated Finline Transition and Low V_{π}," *IEEE Photon. Technol. Lett.*, vol. 11, no. 1, 1999, pp. 54-56.

[10] W. Wang, Y. Shi, D.J. Olson, W. Lin, and J.H. Bechtel, "Push-Pull Poled Polymer Mach-Zëhnder Modulators with a Single Microstrip Line Electrode," *IEEE Photon. Technol. Lett.*, vol. 11, no. 1, 1999, pp. 51-53.

[11] D. An, Z. Shi, L. Sun, J.M. Taboada, Q. Zhou, X. Lu, S. Tang, H. Zhang, W.H. Steier, A. Ren, and L.R. Dalton, "Polymeric Electro-Optic Modulator Based on 1×2 Y-fed Directional Coupler," *Appl. Phys. Lett.*, vol. 76, no. 15, 2000, pp. 1972-1974.

[12] D.H. Chang, H. Erlig, M.C. Oh, C. Zhang, W.H. Steier, L.R. Dalton, and H.R. Fetterman, "Time Stretching of 102-GHz Milimeter Waves Using Novel 1.55-μm Polymer Electrooptic Modulator," *IEEE Photon. Technol. Lett.*, vol. 12, no. 5, 2000, pp. 537-539.

[13] M.C. Oh, H. Zhang, A. Szep, V. Chuyanov, W.H. Steier, C. Zhang, L.R. Dalton, H. Erlig, B. Tsap, and H.R. Fetterman, "Electro-Optic Polymer Modulators for 1.55 μm Wavelength Using Phenyltetraene Bridged Chromophore in Polycarbonate," *Appl. Phys. Lett.*, vol. 76, no. 15, 2000, pp. 3525-3527.

[14] Y. Shi, C. Zhang, H. Zhang, J.H. Bechtel, L.R. Dalton, B.H. Robinson, and W.H. Steier, "Low (Sub-1-Volt) Halfwave Voltages Polymeric Electro-Optic Modulators Achieved by Controlling Chromophore Shape," *SCIENCE*, vol. 288, Apr. 2000, pp. 119-122.

[15] J.I. Thackara, J.C. Chon, G.C. Bjorklund, W. Volksen, and D.M. Burland, "Polymeric Electro-Optic Mach-Zëhnder Switches," *Appl. Phys. Lett.*, vol. 67, no. 26, 1995, pp. 3874-3876.

[16] W.Y. Hwang, M.-C. Oh, H.M. Lee, H. Park, and J.J. Kim, "Polymeric 2×2 Electrooptic Switch Consisting of Asymmetric Y Junctions and Mach-Zëhnder Interferometer," *IEEE Photon. Technol. Lett.*, vol. 9, no. 6, 1997, pp. 761-763.

[17] S.G. Han, H.J. Lee, M.H. Lee, H.J. Lee, H.Y. Kim, and Y.H. Won, "High Performance 2×2 Polymeric Electro-Optic Switch with Modified Bifurcation Optically Active Waveguide Structure," *Electron. Lett.*, vol. 32, no. 21, 10 Oct. 1996, pp. 1994-1995.

[18] M.-H. Lee, Y.H. Min, J.J. Ju, J.Y. Do, and S.G. Park, "Polymeric Electro-optic 2×2 Switch Consisting of Bifurcation Optical Active Waveguides and a Mach-Zëhnder Interferometer," *IEEE J. Selected Topics in Quantum Electron.*, vol. 7, no. 5, 2001, pp. 812-818.

[19] M.-C. Oh, W.-Y. Hwang, and J.J. Kim, "Integrated-Optic Polarization Controlling Devices Using Electro-Optic Polymers," *ETRI J.*, vol. 18, no. 4, Jan. 1997, pp. 287-299.

[20] M. Jager, G.I. Stegerman, S. Yilmaz, W. Wirges, W. Brinker, S. Bauer-Gogonea, S. Bauer, M. Ahlheim, M. Stahelin, B. Zysset, F. Lehr, M. Diemeer, and M.C. Flipse, "Poling and Characterization of Polymer Waveguides for Modal Dispersion Phase-Matched Second-Harmonic Generation," *J. Opt. Soc. Am. B*, vol. 15, no. 2, Feb. 1998, pp. 781-788.

[21] T. Sugihara, H. Haga, S. Yamamoto, "Electrically Tunable Guided-Wave Optical Frequency Converter Using Dye-Doped Polymers," *IEEE J. Lightwave Technol.*, vol. 16, no. 2, Feb. 1998, pp. 239-245.

[22] S. Bauer, "Poled Polymers for Sensors and Photonic Applications," *J. Appl. Phys.*, vol. 80, no. 10, Nov. 1996, pp. 5531-5558.

[23] L. Eldada and L.W. Shacklette, "Advances in Polymer Integrated Optics," *IEEE J. Selected Topics in Quantum Electron.*, vol. 6, Jan/Feb. 2000, pp. 54-68.

[24] Y. Hida, H. Onose, and S. Imamura, "Polymer Waveguide Thermooptic Switch with Low Electric Power Consumption at 1.3 m," *IEEE Photon. Technol. Lett.*, vol. 5, July 1993, pp. 782-784.

[25] N. Keil, H.H. Yao, and C. Zawadzki, "(2×2) Digital Optical Switch Realized by Low Cost Polymer Waveguide Technology," *Electron. Lett.*, vol. 32, no. 16, Aug. 1996, pp. 1470-1471.

[26] M.-C. Oh, H.-J. Lee, M.-H. Lee, J.H. Ahn, and S.G. Han, "Asymmetric X-Junction Thermooptic Switches Based on fluorinated Polymer Waveguides," *IEEE Photon. Technol. Lett.*, vol. 10, June 1998, pp. 813-815.

[27] N. Ooba, S. Toyoda, and T. Kurihara, "Low Crosstalk and Low Loss 1×8 Digital Optical Switch Using Silicone Resin Waveguides," *Electron. Lett.*, vol. 35, no. 16, Aug. 1999, pp. 1364-1365.

[28] S. Toyoda, N. Ooba, Y. Katoh, T. Kurihara, and T. Maruno "Low Crosstalk and Low Loss 2×2 Thermo-Optic Digital Optical Switch Using Silicone Resin Waveguides," *Electron. Lett.*, vol. 36, no. 21, Oct. 2000, pp. 1803-1804.

[29] M.-C. Oh, H.-J. Lee, M.-H. Lee, J.-H. Ahn, S.G. Han, and H.G. Kim, "Tunable Wavelength Filters with Bragg Gratings in Polymer Waveguides," *Appl. Phys. Lett.*, vol. 73, no. 18, Nov. 1998, pp. 2543-2545.

[30] Y.O. Noh, M.-S. Yang, Y.H. Won, and W.-Y. Hwang, "PLC-Type Variable Optical Attenuator Operated at Low Electrical Power," *Electron. Lett.*, vol. 36, no. 24, Nov. 2000, pp. 2032-2033.

[31] M.B.J. Diemmer, L.H. Spiekman, R. Ramsamoedj, and M.K. Smit, "Polymeric Phased Array Wavelength Multiplexer Operating around 1550 nm," *Electron. Lett.*, vol. 32, June 1996, pp. 1132-1133.

[32] S. Toyada, A. Kaneko, N. Ooba, M. Hikita, H. Yamada, T. Kurihara, K. Okamoto, and S. Imamura, "Polarization-Independent Low-Crosstalk Polymeric AWG-Based Tunable Filter Operating Around 1.55 mm," *IEEE Photon. Technol. Lett.*, vol. 11, Sept. 1999, pp. 1141-1143.

[33] J.-H. Ahn, H.-J. Lee, W.-Y. Hwang, M.-C. Oh, M.-H. Lee, S.G. Han, H.-G. Kim, and C.H. Yim, "Polymeric 1×16 Arrayed Waveguide Grating Multiplexer Using Fluorinated Poly(Arylene Ethers) at 1550 nm," *IEICE Trans. Comm.*, vol. E82-B, Feb. 1999, pp. 406-408.

[34] C.C. Tang and H.T. Man, "Simple Reflection Technique for Measuring the Electro-Optic Coefficient of Poled Polymers," *Appl. Phys. Lett.*, vol. 56, no. 18, Apr. 1990, pp. 1734-1736.

[35] C.C. Tang, "Precision Measurements of the Optical Attenuation Profile along the Propagation Path in Thin Film Waveguides," *Applied Optics*, vol. 32, no. 7, Mar. 1993, pp.1051-1054.

[36] Y.H. Min, M.-H. Lee, J.J. Ju, J.Y. Do, and S.G. Park, "Polymeric 16x16 Arrayed Waveguide Grating Router Using Fluorinated Polyethers Operating Around 1550 nm," *IEEE J. Selected Topics in Quantum Electron.*, vol. 7, no. 5, 2001, pp. 806-811.

[37] R. Moosburger and K. Petermann, "4×4 Digital Optical Matrix Switch Using Polymeric Oversized Rib Waveguides," *IEEE Photon. Technol. Lett.*, vol. 10, no. 5, 1998, pp. 684-686.

[38] S. Suzuki, M. Yanagisawa, Y. Hibino, and K. Oda, "High-Density Integrated Plana Lightwave Circuits Using SiO_2-GeO_2 Waveguides with a High Refractive Index Difference," *J. Lightwave Technol.*, vol. 12, May 1994, pp. 790-796.

Myung-Hyun Lee was born in Kyungnam, Korea, on January 22, 1962. He received the BS and MS degrees from Seoul National University, Korea in 1985 and 1987, respectively, and the D. Phil. Degree from Oxford University, UK, in 1993. His thesis research was on the optical properties of nano-sized silver particles. In 1993, he joined Electronics Telecommunications Research Institute (ETRI), Daejeon, Korea, where he worked on the development of photonic switching components. Since 1993, he has been engaged in research on polymeric photonics materials and devices. He is now the Team Leader of the Wideband Photonics Device Team, ETRI.

Jung Jin Ju was born in Kyungnam, Korea, on November 17, 1967. He received the BS, MS and PhD degrees at the Physics Department of Pusan National University, Korea in 1990, 1992 and 1997, respectively. His research in his graduate course was on the laser spectroscopy of rare-earth ions doped solids and the second order nonlinear optics in inorganic crystals. In 1998, he worked at Korea Research Institute of Standards and Science where he researched degenerate four-wave mixing in gas phase. In 1999, he worked at the Electronic Engineering Department of Pohang University of Science and Technology, Korea, where he researched THz generation and detection in semiconductors. In 2000, he joined Electronics Telecommunications Research Institute (ETRI), Daejeon, Korea, where he is working on the development of polymeric waveguide devices based on second order nonlinear optical processes.

Suntak Park received the MS and PhD degrees from the Department of Physics, Hanyang University, Seoul, Korea, in 1997 and 2001, respectively. He is currently a Researcher in the Wideband Photonics Device Team of ETRI. His research interests include polymeric EO devices and surface plasmons.

Jung Yun Do was born in Ulsan, Korea on December 6, 1968. He received the BS from Pusan National University, Korea in 1991, and MS and PhD degrees from Korea Advanced Institute of Science and Technology, Korea in 1993 and 1996, respectively. His main research was on the synthesis of organic molecules and development of synthetic methodology in chemical reaction. He joined Hanwha R&E center in 1996 and Electronics Telecommunications Research Institute (ETRI), Daejeon, Korea, in 1999 where he worked on the development of organic materials for electronic optical components. Since 1999, he has been engaged in research on polymeric photonic materials and devices.

Seung Koo Park was born in Seoul, Korea, on May 20, 1963. He received his BS, MS, and PhD degrees from Seoul National University, Korea in 1986, 1993, and 1997, respectively. He is interested in polyimide synthesis and modification. He worked for Dr. Farris at the University of Massachusetts at Amherst as a Post-Doc. for 3 years to develop fire-safe polymers. Since July 2000, he has worked for Wideband Photonic Device Team, Electronics Telecommunications Research Institute, Daejeon, Korea, and investigated a new polymer system for electro and nonlinear optic materials.